Alternative Pathways and Reactions of Benzyl Alcohol and Benzaldehyde with Horse Liver Alcohol Dehydrogenase†

Gretchen L. Shearer, Keehyuk Kim, Kang Man Lee,‡ C. Kathy Wang,§ and Bryce V. Plapp*

Department of Biochemistry, The University of Iowa, Iowa City, Iowa 52242

Received June 1, 1993; Revised Manuscript Received August 4, 1993⊕

ABSTRACT: Liver alcohol dehydrogenase catalyzes the reaction of NAD^+ and benzyl alcohol to form NADH and benzaldehyde by a predominantly ordered reaction. However, enzyme–alcohol binary and abortive ternary complexes form at high concentrations of benzyl alcohol, and benzaldehyde is slowly oxidized to benzoic acid. Steady-state and transient kinetic studies, equilibrium spectrophotometric measurements, product analysis, and kinetic simulations provide estimates of rate constants for a complete mechanism with the following reactions: (1) $E \rightleftharpoons E\text{–}NAD^+ \rightleftharpoons E\text{–}NAD^+\text{–}RCH_2OH \rightleftharpoons E\text{–}NADH\text{–}RCHO \rightleftharpoons E\text{–}NADH \rightleftharpoons E$; (2) $E\text{–}NADH \rightleftharpoons E\text{–}NADH\text{–}RCH_2OH \rightleftharpoons E\text{–}RCH_2OH \rightleftharpoons E$; (3) $E\text{–}NAD^+ \rightleftharpoons E\text{–}NAD^+\text{–}RCHO \rightarrow E\text{–}NADH\text{–}RCOOH \rightleftharpoons E\text{–}NADH$. The internal equilibrium constant for hydrogen transfer determined at 30 °C and pH 7 is about 5:1 in favor of $E\text{–}NAD^+\text{–}RCH_2OH$ and has a complex pH dependence. Benzyl alcohol binds weakly to free enzyme (K_d = 7 mM) and significantly decreases the rates of binding of NAD^+ and NADH. The reaction of NAD^+ and benzyl alcohol is therefore kinetically ordered, not random. High concentrations of benzyl alcohol (>1 mM) inhibit turnover by formation of the abortive $E\text{–}NADH\text{–}RCH_2OH$ complex, which dissociates at 0.3 s^{-1} as compared to 6.3 s^{-1} for E–NADH. The oxidation of benzaldehyde by $E\text{–}NAD^+$ (K_m = 15 mM, V/E = 0.4 s^{-1}) is inefficient relative to the oxidation of benzyl alcohol (K_m = 28 μM, V/E = 3.1 s^{-1}) and leads to a dismutation ($2RCHO \rightarrow RCH_2OH + RCOOH$) as E–NADH reduces benzaldehyde. The results provide a description of final product distributions for the alternative reactions catalyzed by the multifunctional enzyme.

The mechanism of horse liver alcohol dehydrogenase is classically described as ordered bi bi, but random addition of substrates and abortive complexes have been described (Dalziel & Dickinson, 1966a,b; Ainslie & Cleland, 1972). The enzyme can also oxidize aldehydes to acids by a dismutation (Abeles & Lee, 1960; Dalziel & Dickinson, 1965; Hinson & Neal, 1972, 1975; Battersby et al., 1979; Anderson & Dahlquist, 1982a; Henehan & Oppenheimer, 1993). Rate constants for all steps of the various reactions should be determined for a quantitative description of the mechanism.

The on-enzyme or internal equilibrium constant, K_{int}, for the hydrogen-transfer step is of interest because of the proposal that efficient enzymes shift the equilibrium constant for bound substrates toward 1 (Albery & Knowles,1976; Burbaum et al., 1989; Burbaum & Knowles, 1989). Direct spectrophotometric measurements with liver alcohol dehydrogenase gave a value of about 1 (Theorell & Yonetani, 1962), but transient kinetics and NMR results suggest that K_{int} is about 10:1 in favor of the enzyme–NAD^+–alcohol complex (McFarland & Chu, 1975; Jacobs et al., 1974; Anderson & Dahlquist, 1980; Nambiar et al., 1983; Sekhar & Plapp, 1990). K_{int} could be affected by pH, since the pH dependence of the transient oxidation of alcohol shows a pK value near 7 and a proton is a product (Theorell & Yonetani, 1962; Brooks et al., 1972; Shore et al., 1974; Kvassman & Pettersson, 1978; Sekhar & Plapp, 1988).

X-ray crystallography data for horse liver alcohol dehydrogenase crystallized with NAD^+ and *p*-bromobenzyl alcohol have been interpreted as if the complex were enzyme–NAD^+–alcohol (Eklund et al., 1982), but direct microspectrophotometric determinations suggested that most of the coenzyme was NADH (Bignetti et al., 1979). Schneider et al. (1985) suggested that the complex is an abortive complex with NADH and the alcohol, but no data or mechanism for NADH formation was presented. NADH could be produced if the alcohol were oxidized to aldehyde and then to the acid.

The purpose of this work is to describe a complete mechanism for the enzyme acting on benzyl alcohol and benzaldehyde, to determine K_{int} and its pH dependence, to evaluate the significance of random pathways and abortive complexes, and to describe the composition of the equilibrium mixture of enzyme, coenzyme, and substrate. Our experimental approach uses simulation of the progress curves for the various reactions, so that all kinetic and equilibrium data are integrated in one mechanism.

EXPERIMENTAL PROCEDURES

Materials. Crystalline horse liver alcohol dehydrogenase obtained from Boehringer-Mannheim was freed of ethanol by gel filtration through Sephadex G-50 or by dialysis and was clarified by centrifugation. The concentration of protein was determined by UV absorption (A_{280} = 0.455/cm for 1 mg/mL). The concentration of active sites (normality) was determined by titration with NAD^+ in the presence of 10 mM pyrazole (Theorell & Yonetani, 1963). The enzyme was homogeneous by electrophoresis and chromatography; 95% of the subunits could bind NAD^+. At 30 °C, the enzyme has a turnover number of 2.3 s^{-1} (3.5 units/mg) as assayed by a standard procedure (Plapp, 1970). $LiNAD^+$ (grade I) and Na_2NADH (grade I) were obtained from Boehringer-Mannheim. Benzyl alcohol and benzaldehyde were redistilled

† This work was supported by Grant AA00279 from the National Institute on Alcohol Abuse and Alcoholism, U.S. Public Health Service.

* Author to whom correspondence should be addressed: Department of Biochemistry, 4-370 Bowen Science Bldg., The University of Iowa, Iowa City, IA 52242.

‡ Visiting Scientist from College of Pharmacy, Ewha Woman's University, Seoul, Korea.

§ Present address: The Rockefeller University, New York, NY.

⊕ Abstract published in *Advance ACS Abstracts,* October 1, 1993.

0006-2960/93/0432-11186$04.00/0

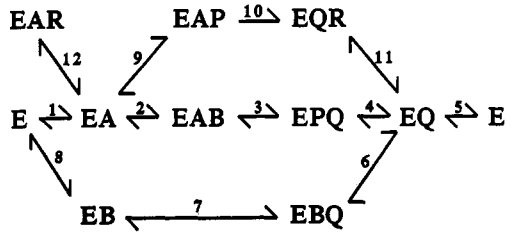

FIGURE 1: Mechanism for liver alcohol dehydrogenase acting on benzyl alcohol and benzaldehyde, including the substrate inhibition pathway and the dismutation reaction. E represents enzyme, A is NAD^+, B is benzyl alcohol, Q is NADH, P is benzaldehyde, and R is benzoic acid. The step numbers correspond to the kinetic constants listed in Table III.

before use. [α-^{13}C]Benzyl alcohol (99%) was obtained from MSD Isotopes.

Kinetic Studies. Initial velocities were determined with a Cary 118C spectrophotometer interfaced to a Data Translation A/D board in an IBM PC/XT by fitting the time courses to a straight line or a parabola with a Fortran program. Kinetic studies were also carried out using an SLM Aminco 4800 fluorometer, and the initial velocity data were fit to a straight line or parabola with a least-squares analysis program provided with the instrument software. The buffers used were 50 mM sodium *N*-[tris(hydroxymethyl)methyl]-2-aminoethanesulfonate (TES[1]) or 46 mM sodium phosphate and 0.25 mM EDTA (pH 7.0). Steady-state data were analyzed with the Fortran programs of Cleland (1979). A BioLogic SFM3 stopped-flow instrument with three syringes for variation of the concentrations of reactants and a dead-time determined to be 2.5 ms was used to measure the transient reactions. The BioKine Software was used for data analysis. Some preliminary experiments used a Kinetic Instruments stopped-flow apparatus with a dead-time of 1.3 ms, designed by Dr. David P. Ballou, and software from On-Line Instruments Systems (Bogart, GA). For transient kinetics and equilibrium studies, an extinction coefficient of 5500 $M^{-1}cm^{-1}$ at 328 nm was used for the difference in absorption of NADH and NAD^+ bound to enzyme and its complexes (Theorell & Bonnichsen, 1951; Baici & Luisi, 1977; Andersson & Pettersson, 1982). The kinetic simulation program, KINSIM, and an automatic fitting routine, FITSIM, were used to estimate rate constants for the overall enzymatic reaction by fitting several progress curves simultaneously (Barshop et al., 1983; Zimmerle & Frieden, 1989).

NMR spectra were obtained on a Bruker WM360 NMR instrument with a 10-mm, broad-band probe. The recycle time was 2.7 s; 3000 scans were accumulated and processed with 20-Hz line broadening.

RESULTS

Overview. The mechanism in Figure 1 describes the results given below for the reactions of benzyl alcohol and benzaldehyde with coenzyme and liver alcohol dehydrogenase, including the dismutation and a pathway containing the enzyme–NADH–alcohol complex. Some of the rate and equilibrium constants for this mechanism were directly determined by the steady-state and transient studies. Other rate constants were estimated by the simulation of progress curves for the forward and reverse reactions. The full mechanism was described in a stepwise fashion. The rates of binding and dissociation of NAD^+ and NADH were determined by transient kinetics and fixed in all subsequent simulations. The ordered mechanism (steps 1–5) was simulated using progress curves collected at high concentrations of NAD^+ or NADH and noninhibitory concentrations (<1 mM) of benzyl alcohol and benzaldehyde. The kinetic constants were then fixed in simulations of the abortive pathway (steps 6–8) for progress curves at high concentrations of benzyl alcohol and varied concentrations of NAD^+. Several different mechanisms for the substrate inhibition were tested, including ones with simple deadend enzyme–alcohol and enzyme–NADH–alcohol complexes. After the constants for the ordered bi bi mechanism and the abortive complex pathways were determined, the dismutation was simulated.

Table I: Kinetic Constants for Liver Alcohol Dehydrogenase Acting on Benzyl Alcohol and Benzaldehyde[a]

constant	value	constant	value
K_a, μM	3.7	K_{iq}, μM	0.41
K_b, μM	28	K_bK_{ia}/K_a, μM	420
K_p, μM	120	K_pK_{iq}/K_q, μM	6.8
K_q, μM	9.9	V_1, s^{-1}	3.1
K_{ia}, μM	120	V_2, s^{-1}	110
K_{ib}, μM	240	K_{eq}^{I}, pM	38
K_{ip}, μM	26	K_{eq}^{II}, pM	20

[a] Product inhibition studies, as described by Dworschack and Plapp (1977), were used at 30 °C. The buffer was 50 mM sodium TES and 0.25 mM EDTA (pH 7.0) for the reverse reaction and 46 mM sodium phosphate (pH 7.0) for the forward reaction. Studies in the forward reaction used the SLM fluorometer, whereas the reverse reaction was measured spectrophotometrically. Kinetic constants are for an ordered bi bi mechanism, where K_a, K_b, K_p, and K_q are the Michaelis constants for NAD^+, benzyl alcohol, benzaldehyde, and NADH, respectively. V_1 is the turnover number for benzyl alcohol oxidation, and V_2 is the turnover number for benzaldehyde reduction. Corrections for nonsaturation of fixed substrate used the equations in Plapp (1970). Standard errors of fits were less than 20% of the listed values. K_{eq}^{I} and K_{eq}^{II} are the equilibrium constants calculated from the Haldane relationship (Cleland, 1963). Values for the equilibrium constant have been estimated to be 20–60 pM (Bernhard et al., 1970; Klinman, 1972; Luisi & Bignetti, 1974; Weidig et al., 1977; Dunn et al., 1979). We determined a value of 24 pM at 25 °C by finding ratios of substrate concentrations that gave no net change in coenzyme upon the addition of catalytic levels of enzyme.

Ordered Bi Bi Mechanism. Steady-state initial velocity and product inhibition kinetics with low concentrations of benzyl alcohol are consistent with an ordered bi bi mechanism, as reported in many previous studies. The kinetic constants derived from product inhibition studies reported in (Table I) provide the fundamental parameters for the mechanism. The rates for coenzyme binding and dissociation were obtained as described by Sekhar and Plapp (1988). The values given in Table II were fixed in all subsequent simulations.

Transient data were collected with 10 μN enzyme and 1 mM NAD^+ and varied concentrations of benzyl alcohol (0.04–0.50 mM) or 11 μM NADH and benzaldehyde (0.02–0.1 mM), and the reaction curves were simulated with FITSIM to obtain estimates of the rate constants for steps 2–4 in Figure 1 (Table III). Benzyl alcohol is oxidized in an initial exponential phase controlled by hydride transfer, followed by a steady-state increase in absorbance at 328 nm controlled by the rate of dissociation of NADH (Theorell & Chance, 1951; Dalziel, 1963). The initial phase was first order with a maximal rate constant of 22 s^{-1} at saturating alcohol levels. The maximal amplitude of the exponential phase was about 60% of that expected on the basis of the active enzyme concentration. The transient reduction of benzaldehyde was first order with a maximal rate constant of 200 s^{-1} at saturating benzaldehyde. The results were similar to those obtained using 20 mM pyrazole to trap the enzyme–NAD^+ complex (Sekhar & Plapp, 1988). The amplitudes in the reverse direction were

[1] Abbreviations: TES, *N*-[tris(hydroxymethyl)methyl]-2-aminoethanesulfonate.

Table II: Rate Constants for Binding of NAD^+ and NADH[a]

$$E \underset{k_{-1}}{\overset{k_1}{\rightleftharpoons}} E\text{–}NAD^+ \underset{k_{-1}^*}{\overset{k_1^*}{\rightleftharpoons}} F\text{–}NAD^+ \underset{k_{-13}}{\overset{k_{13}}{\rightleftharpoons}} F\text{–}NAD^+\text{–pyrazole} \qquad E\text{–}NADH \underset{k_{-5}}{\overset{k_5}{\rightleftharpoons}} E$$

$k_1 = 36 \times 10^6\ M^{-1}\ s^{-1}$	$k_{-1} = 22000\ s^{-1}$
$k_1^* = 880\ s^{-1}$	$k_{-1}^* = 190\ s^{-1}$
$k_{13} = 1.2 \times 10^6\ M^{-1}\ s^{-1}$	k_{-13} was fixed at $0.01\ s^{-1}$
$k_5 = 6.3\ s^{-1}$	$k_{-5} = 21 \times 10^6\ M^{-1}\ s^{-1}$

[a] The rate constants for NAD^+ binding and dissociation were obtained as described by Sekhar and Plapp (1988) at pH 7 and 30 °C, in 46 mM sodium phosphate buffer. The observed rate constants for varied concentrations of NAD^+ and pyrazole were fit by SEQUEN with the maximum isomerization rate of 890 (±130) s^{-1} and a k_{on} for NAD^+ of $(2.1 \pm 0.3) \times 10^6\ M^{-1}\ s^{-1}$. The progress curves were best simulated using the mechanism given above, which includes the isomerization of E–NAD^+ to F–NAD^+. The standard errors of the fitted parameters were less than 15%. Since the isomerization rate is over 100 times faster than the rate-limiting release of NADH, the overall rate constants for NAD^+ binding were calculated from the rate constants, and the isomerization step was not included in the simulations of the full mechanism. The calculated $k_{on}\,[k_1k_1^*/(k_{-1} + k_1^*)]$ is $1.4 \times 10^6\ M^{-1}\ s^{-1}$ and the $k_{off}\,[k_{-1}k_1^*k_{-1}^*/(k_{-1} + k_1^*)(k_1^* + k_{-1}^*)]$ is $150\ s^{-1}$. The rate of NADH binding was determined by following the fluorescence quenching of the protein mixed in a 1:1 ratio with NADH (see Figure 4A). The rate of dissociation of NADH was determined by mixing 10 μM enzyme–NADH with varied concentrations (0.1–1.0 mM) of NAD^+ at 2.5 and 5 mM pyrazole and following the formation of the enzyme–NAD^+–pyrazole complex at 294 nm (ϵ = 9000 $M^{-1}\ cm^{-1}$). The errors for NADH binding rate constants were less than 10% of the values.

Table III: Rate Constants for a Mechanism Including Abortive Ternary Complexes and the Dismutation[a]

step	reaction	forward (k_n)	reverse (k_{-n})
1	E + A ⇌ EA	$1.4 \times 10^6\ M^{-1}\ s^{-1}$ [b]	$150\ s^{-1}$ [b]
2	EA + B ⇌ EAB	$3.2 \times 10^6\ M^{-1}\ s^{-1}$	$85\ s^{-1}$
3	EAB ⇌ EPQ	$47\ s^{-1}$	$240\ s^{-1}$
4	EPQ ⇌ EQ + P	$79\ s^{-1}$	$2.8 \times 10^6\ M^{-1}\ s^{-1}$
5	EQ ⇌ E + Q	$6.3\ s^{-1}$ [b]	$2.1 \times 10^7\ M^{-1}\ s^{-1}$ [b]
6	EQ + B ⇌ EBQ	$5.2 \times 10^6\ M^{-1}\ s^{-1}$	$3300\ s^{-1}$
7	EBQ ⇌ EB + Q	$0.32\ s^{-1}$	$3.4 \times 10^6\ M^{-1}\ s^{-1}$ [c]
8	EB ⇌ E + B	$7.9 \times 10^4\ s^{-1}$ [d]	$1.1 \times 10^7\ M^{-1}\ s^{-1}$ [d]
9	EA + P ⇌ EAP	$4.0 \times 10^7\ M^{-1}\ s^{-1}$	$1.0 \times 10^5\ s^{-1}$
10	EAP ⇌ EQR	$0.38\ s^{-1}$	$1.0 \times 10^{-9}\ s^{-1}$ [e]
11	EQR ⇌ EQ + R	$1.5 \times 10^6\ s^{-1}$ [f]	$1.0 \times 10^7\ M^{-1}\ s^{-1}$ [f]
12	EA + R ⇌ EAR	$1.0 \times 10^6\ M^{-1}\ s^{-1}$ [g]	$1.4 \times 10^4\ s^{-1}$ [g]

[a] Estimates are derived from kinetic simulations of transient reactions as described in the text. Standard errors are less than 15%, and cumulative errors are 2–3-fold, as compared to the overall equilibrium constant. [b] Coenzyme binding and dissociation rates (given in Table II) were fixed throughout the simulations. [c] This value was determined from NADH binding to the E–alcohol complex (Figure 4B) and fixed in the simulation of the abortive pathway. [d] Rate constants in both directions were simulated in a fixed ratio of 7.2 mM, which was determined experimentally (Figure 4B). [e] The oxidation of benzaldehyde to benzoic acid is irreversible, so that a very small rate constant was fixed for the simulation of the dismutation. [f] The rate constants were chosen arbitrarily such that the ratio is equivalent to the K_d of 150 ± 30 mM reported in the literature (Andersson et al., 1981). [g] The rate constants were chosen arbitrarily such that the ratio is equivalent to the K_d determined experimentally in this work, 14 mM.

about 80% of those expected for the concentration of enzyme. The description of these reactions as first order does not imply that the transient reactions are monophasic, as biphasic kinetics are predicted from the equations for the ordered mechanism (Pettersson, 1976) and have been studied extensively (Bernhard et al., 1970; McFarland & Bernhard, 1972; Luisi & Bignetti, 1974; Hadorn et al., 1975; Dunn et al., 1979; Kvassman & Pettersson, 1976; Weidig et al., 1977; Baici & Luisi, 1977; Anderson & Dahlquist, 1982b; Andersson & Pettersson, 1982). Rather than attempting to resolve the possible phases, we fit the data to the complete mechanism with kinetic simulation. The transient reactions are described

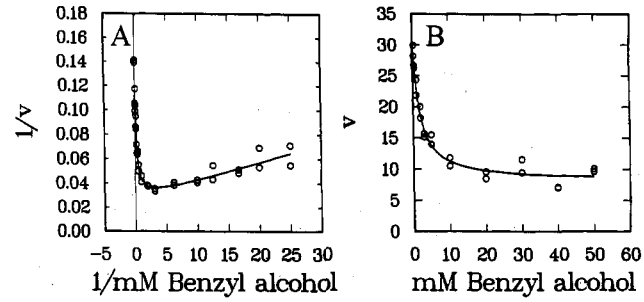

FIGURE 2: Substrate inhibition by benzyl alcohol. The activity of 32 nN alcohol dehydrogenase was determined with 0.75 mM NAD^+ and 0.04–50 mM benzyl alcohol in 50 mM sodium TES buffer, pH 7.0, at 30 °C. Velocities in units of ΔA_{340}/min have been multiplied by 1000. (A) The data were fit with the TWOONE equation (Cleland, 1979), $v = V(dB + B^2)/(c + bB + B^2)$, with estimates of $V = 8.2 \pm 0.6$, $b = 1.1 \pm 0.2$ mM, $c = 0.065 \pm 0.009$ mM^2, and $d = 5.2 \pm 1.2$ mM, for the mechanism in Scheme I. (B) The data for benzyl alcohol concentrations from 0.32 to 50 mM (substrate concentrations much larger than the apparent K_m of 0.043 mM) were fit to the HYPRPLT equation, $v = V(1 + B/K_{in})/(1 + B/K_{id})$ where $K_{in} = k_5K_{qb}/k_7 = 6.0 \pm 1.1$ mM, $K_{id} = K_{qb} = 1.4 \pm 0.3$ mM, and $V = 33.3 \pm 1.5$.

Scheme I

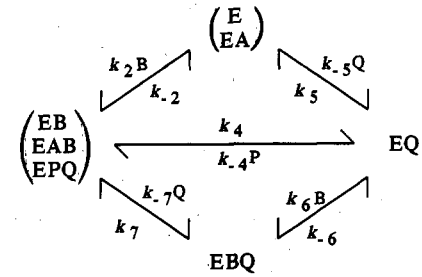

and fit well by the ordered bi bi mechanism given in Figure 1 and the rate constants for steps 1–5 in Table III, as illustrated previously (Lee et al., 1988; Sekhar & Plapp, 1988, 1990; Plapp et al., 1993). Interacting subunits are not required to explain the biphasic kinetics.

Substrate Inhibition and Abortive Complexes. High concentrations of benzyl alcohol produce substrate inhibition in initial velocity studies (Figure 2A). Previous work established that inhibition by ethanol or activation by cyclohexanol is due to the formation of an abortive enzyme–NADH–alcohol complex, from which NADH dissociates either faster or slower than it does for the binary enzyme–NADH complex (Dalziel & Dickinson, 1966a,b). The data in Figure 2A can be described by a simple mechanism derived from the one in Figure 1, when NAD^+ levels are saturating and with some reasonable assumptions about the relative magnitudes of the rate constants.

If we assume that $k_{-6} \gg k_7$ and $k_4 \gg k_5$ or k_7 (Scheme I), the following equation is derived:

$$v = \frac{k_7V/k_5(K_{qb}k_5B/k_7 + B^2)}{K_bK_{qb} + (k_{-2}k_7/k_2k_4 + K_{qb})B + B^2} \qquad (1)$$

where K_b is the Michaelis constant for alcohol $[k_5(k_{-2} + k_4)/k_2(k_5 + k_4)]$ and K_{qb} is the dissociation constant for alcohol from the enzyme–NADH–alcohol complex, i.e., k_{-6}/k_6. This equation has the same form as the TWOONE function (Cleland, 1979), which was used to fit the data in Figure 2A. This analysis gave $K_{qb} = 1.4$ mM, $k_5/k_7 = 4$, and $K_b = 46$ μM. Alternatively, if we consider only the data for concentrations of alcohol much higher than K_b, so that terms containing K_b are eliminated, the data (Figure 2B) are described by a

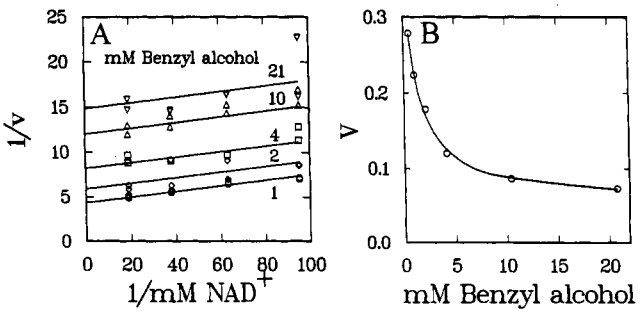

FIGURE 3: Hyperbolic uncompetitive substrate inhibition by benzyl alcohol against NAD^+. (A) Enzyme concentration was 22 nN, and the buffer was 50 mM sodium TES and 0.25 mM EDTA (pH 7.0, 30 °C). The initial velocities (ΔF/min) were determined on the fluorometer with excitation at 340 nm and emission at 460 nm. The data were fit to the equation for hyperbolic uncompetitive inhibition: $v = V_mA/K_m + A((1 + I/K_{in})/(1 + I/K_{id}))$ where $V_m = 0.41 \pm 0.06$ s^{-1}, $K_m = 13 \pm 3$ μM, $K_{in} = K_{qb} = 1.0 \pm 0.3$ mM, and $K_{id} = 8.4 \pm 2.3$ mM. (B) V_m values obtained from the fit to HYPER for each benzyl alcohol concentration in A were fit with the hyperbolic replot equation as in Figure 2B, where $V_m = 0.37 \pm 0.01$, $K_{in} = K_{qb} = 1.2 \pm 0.1$ mM, and $K_{id} = 8.7 \pm 0.6$ mM.

Scheme II

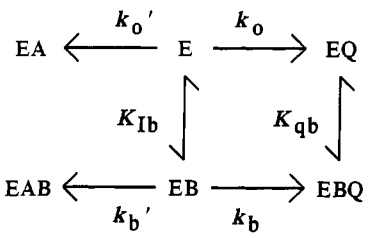

hyperbolic function of the observed velocity against alcohol concentration and may be fit with HYPRPLT (Cleland, 1979) to give a value of $K_{qb} = 1.4$ mM.

If the inhibition by benzyl alcohol is due to formation of an abortive enzyme–NADH–alcohol complex that releases NADH more slowly than does enzyme–NADH, high concentrations of benzyl alcohol should produce hyperbolic uncompetitive substrate inhibition. The data (Figure 3A) are consistent with the proposed mechanism ($K_{qb} = 1.0$ mM) and show that deadend EB or EAB_2 complexes are not significant over the range of concentrations used. The binding of pentafluorobenzyl alcohol to the enzyme–NADH complex was also measured directly by titrating the complex and following the quenching of NADH fluorescence at 440 nm with excitation at 340 nm. The hyperbolic saturation gave a dissociation constant of 0.82 ± 0.03 mM.

The benzyl alcohols also decreased the rates of binding of NADH and NAD^+ as determined by stopped-flow kinetics. The results are described by the mechanism in Scheme II. The rate constant for binding NADH decreased 6-fold upon formation ($K_{Ib} = 7.2$ mM) of the enzyme–alcohol complex (Figure 4). Andersson et al. (1984b) also obtained a value of 7 mM at 25 °C and found that binding was independent of pH in the range of 6–10.

Benzyl alcohol binds to free enzyme, and it has been assumed that NAD^+ binds to the enzyme–alcohol complex. This was tested by determining the rate of NAD^+ binding to the enzyme–pentafluorobenzyl alcohol complex, which gave a value of about 4000 M^{-1} s^{-1}, indicating that NAD^+ does not bind to the enzyme–benzyl alcohol complex or that it binds very slowly (Figure 5). Andersson et al. (1984b) also found that the binding of NAD^+ was slower by at least an order of magnitude when the enzyme was complexed with 2,2,2-trifluoroethanol.

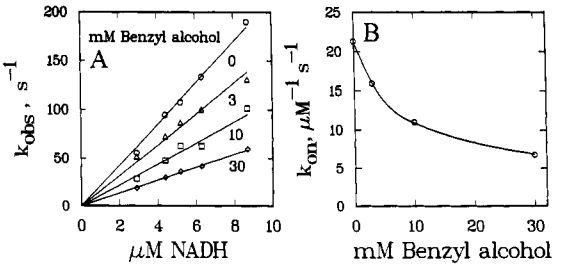

FIGURE 4: NADH binding to enzyme–benzyl alcohol complex. (A) Enzyme preincubated with varied concentrations of benzyl alcohol was mixed with NADH in an equimolar ratio in 46 mM sodium phosphate and 0.25 mM EDTA (pH 7) at 30 °C. The transient was followed by quenching of protein fluorescence with excitation at 294 nm and emission at 330 nm, and the curves fit a second-order equation. Rate constants as a function of NADH concentration were fit by linear regression. (B) The bimolecular rate constants were fit to the equation $k_{obs} = (k_o + k_bB/K_{Ib})/(1 + B/K_{Ib})$, to estimate the rate constant for binding of NADH to enzyme–benzyl alcohol (at saturating [B]) as (3.4 ± 0.4) × 10^6 M^{-1} s^{-1}, and a dissociation constant, K_{Ib}, for B from EB as 7.2 ± 0.5 mM, as defined in Scheme II.

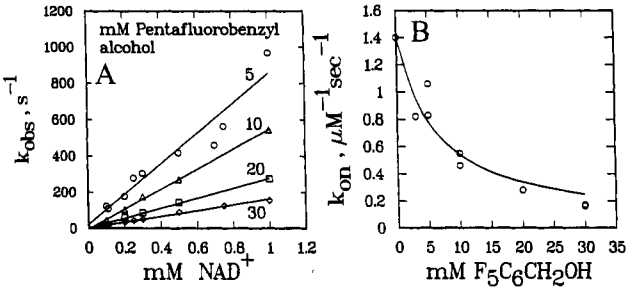

FIGURE 5: NAD^+ binding to enzyme–pentafluorobenzyl alcohol complex. (A) NAD^+ binding was measured with 4 μN enzyme and varied concentrations of NAD^+ and pentafluorobenzyl alcohol in 46 mM sodium phosphate buffer and 0.25 mM EDTA (pH 7) at 30 °C. Quenching of protein fluorescence was measured with excitation at 294 nm and emission at 330 nm. Transient curves fit a first-order reaction, and the rate constants obtained at varied concentrations of NAD^+ were fit using linear regression. (B) The bimolecular rate constants were analyzed with the equation given in Figure 4B, which yielded a poorly defined rate constant for NAD^+ binding to the enzyme–benzyl alcohol complex of 4000 M^{-1} s^{-1} and a dissociation constant for the binary complex (K_{Ib}) of 4.9 ± 0.7 mM.

Simulation of the Abortive Complex Pathway. Transient data were collected at inhibitory concentrations (0.7–50 mM) of benzyl alcohol and varied NAD^+ concentrations (0.33–1 mM). These reaction curves, and those collected at low concentrations of benzyl alcohol and benzaldehyde, were simulated with several possible abortive pathways, with fixed values for steps 1–5. The best fit was obtained with the mechanism shown in Figure 1. The data were also fit with a mechanism that included a step where NAD^+ binds to the enzyme–benzyl alcohol complex, but the dissociation constant obtained from the simulation for this step was 3 orders of magnitude larger than that suggested by the linked equilibria in steps 1, 2, and 8. Furthermore, the poorly determined estimate of the rate constant for association was 12 000 M^{-1} s^{-1}, which would make the step kinetically insignificant.

For the mechanism in Figure 1, the simulated rate constant for dissociation of NADH from the enzyme–NADH–benzyl alcohol complex was 0.3 s^{-1}, which agrees well with the estimate of 0.4 s^{-1} from the steady-state data. Kamlay and Shore (1983) found that bound ethanol decreased the rate of dissociation of NADH by 4-fold. Alcohol dissociates from the enzyme–NADH–alcohol complex (step 6) with a constant estimated to be 1.2 mM from the steady-state inhibition studies (Figures 2 and 3) and 0.8 mM from direct binding experiments. When

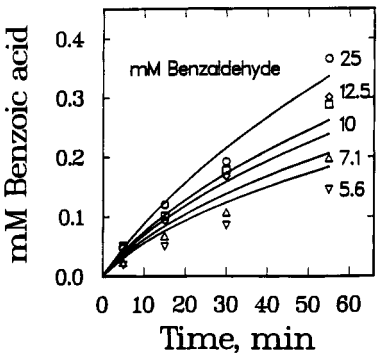

FIGURE 6: Benzaldehyde oxidation. The assays were carried out at 5.6, 7.1, 10, 12, and 25 mM benzaldehyde with 1.0 mM NAD^+, 0.5 μN enzyme, and 50 mM sodium TES (pH 7.0, 30 °C). An aliquot of the reaction solution was removed before addition of the enzyme and added to the quench solution in order to estimate the benzoic acid in the benzaldehyde. After addition of the enzyme, aliquots were removed at 5, 15, 30, and 55 min of reaction time, and the reaction was quenched in the solvent system for HPLC. The composition of reaction mixtures was determined using an Altex Ultrasphere octyl column (4.6 mm × 25 cm) and a 5-cm guard column filled with LC8 pellicular packing (Supelco) developed with acetonitrile/acetic acid/water (30:1:69). The Millipore Waters LC detector was set at 254 nm. Benzyl alcohol, benzoic acid, and benzaldehyde were well resolved with elution times of 7, 9, and 13 min, respectively. Areas under the peaks were integrated with a Hewlett-Packard 3388A integrator. The data points are an average of duplicate assays. The apparent K_m was 15 ± 2 mM, the turnover number was 0.4 ± 0.1 s^{-1}, and the V/K_m was 26 ± 5 M^{-1} s^{-1}. For comparison, the constants for benzyl alcohol oxidation and benzaldehdye reduction are listed in Table I. The dismutation reactions were simulated using the mechanism shown in Figure 1. The lines shown in the figure are kinetic simulations, and the microscopic rate constants are given in Table III.

the association and dissociation rate constants were not fixed, the simulation gave a ratio for k_{-6}/k_6 of 0.6 mM, which agrees well with the values from other experimental determinations. The dissociation constant for the enzyme–alcohol complex (step 8) determined from the stopped-flow experiment was 7.2 mM, and the data were simulated well with k_{-8}/k_8 fixed in this ratio. The values obtained are given in Table III.

Dismutation Reactions. Liver alcohol dehydrogenase can oxidize aldehydes to the acid with NAD^+, but kinetic data for benzaldehyde have not been reported. The oxidation of aldehyde produces NADH, which reduces another molecule of aldehyde, leading to a dismutation that occurs with no net change in coenzyme oxidation.

$$RCHO + E\text{–}NAD^+ \rightarrow RCOOH + E\text{–}NADH$$

$$RCHO + E\text{–}NADH \rightarrow RCH_2OH + E\text{–}NAD^+$$

$$2RCHO \rightarrow RCH_2OH + RCOOH$$

The kinetic parameters for benzaldehyde dismutation were determined by measuring the production of benzyl alcohol and benzoic acid (Figure 6). The rates of production of acid and alcohol were equal within experimental error, as required by the stoichiometry of the dismutation. The data were simulated using the mechanism in Figure 1. The fitted curves are shown in Figure 6, and the rate constants are listed in Table III.

Benzoate is not reduced by NADH, but it binds to the enzyme–NADH complex with a K_i of 150 (±30) mM (Andersson et al., 1981). It is also a competitive inhibitor against ethanol or benzyl alcohol, with a dissociation constant of 14 (±3) mM with 1 mM NAD^+ in 46 mM sodium phosphate buffer and 0.25 mM EDTA (pH 7) at 30 °C.

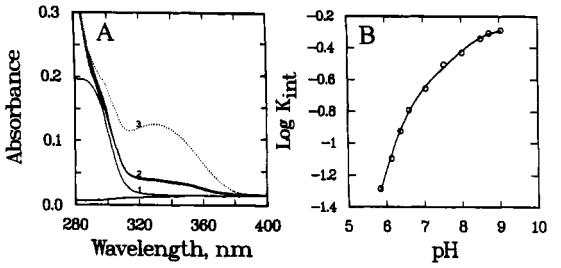

FIGURE 7: Spectrophotometric determination and pH dependence of internal equilibrium. (A) 25 μN enzyme was mixed with 1.0 mM benzyl alcohol and 0.1 mM benzaldehyde, at pH 7.05 and 30 °C, and spectrum (1) was taken; then NAD^+ (to 25 μM) was added and several spectra (2) were recorded over 42 min. Finally, isobutyramide (to 0.1 M) was added and spectrum (3) recorded. (B) pH dependence. Enzyme stock solution (approximately 1.15 mN) was prepared from crystalline enzyme by dialysis in 1 mM sodium phosphate buffer containing 0.1 M sodium sulfate (pH 7.1) and diluted into various 33 mM sodium phosphate buffers to give final pH values from 5.85 to 9.04. The equilibrium mixture contained 25 μN enzyme, 25 μM NAD^+, 1 mM benzyl alcohol, and 0.1 mM benzaldehyde in a 10-mm cuvette at 25 °C. The reference cuvette contained 25 μN enzyme. The total concentration of coenzyme available for reduction to NADH was determined by adding isobutyramide to 0.1 M after 30 min of reaction at pH 8.7. K_{int} was calculated as $A_{328}/(A_{final} - A_{328})$. The pH dependence is described by the mechanism in Scheme III and the equation $K_{int,app} = (k_a + k_x K_2/[H^+])/(1 + [H^+]/K_1 + K_2/[H^+])$, where $k_a = 0.260 \pm 0.008$, $k_x = 0.538 \pm 0.009$, $pK_1 = 6.48 \pm 0.05$, and $pK_2 = 8.11 \pm 0.15$.

Equilibrium Studies. When the enzyme was mixed with NAD^+ and benzyl alcohol, the absorbance at 328 nm increased, consistent with the formation of NADH which absorbs maximally at 325 nm in the enzyme complex (Theorell & Bonnichsen, 1951). The magnitude of the increase was much less than would be expected if all of the bound coenzyme were converted to NADH. There was often a slow increase in absorbance occurring over some minutes, which was also observed by Theorell and Yonetani (1962). The slow reaction could be due to the dismutation or other reaction of aldehyde, resulting in the formation of more NADH, which is firmly bound to the enzyme. When enzyme was mixed with saturating levels of alcohol and aldehyde and then mixed with NAD^+, more stable spectra were obtained, as shown in Figure 7A. The experiment was designed to use stoichiometric concentrations of enzyme and coenzyme and to drive all of the enzyme into ternary complexes with high concentrations of substrates. The initial absorbance at 328 nm reflects the fraction of ternary complexes present as enzyme–NADH–aldehyde. The total concentration of coenzyme that was reducible to NADH was determined by adding isobutyramide to the reaction mixture, trapping the NADH as the tight enzyme–NADH–isobutyramide complex (Theorell & McKinley-McKee, 1961). The difference between the total coenzyme concentration and the concentration of NADH before the addition of isobutyramide represents the concentration of NAD^+ at equilibrium. The NADH to NAD^+ ratio gives an estimate of K_{int}. At pH 7.0 and 25 °C, about 20% of the coenzyme is NADH, corresponding to a K_{int} of 0.25. Similar results were obtained at 30 °C and when the concentrations of benzyl alcohol and benzaldehyde were lowered to 0.2 and 0.02 mM. The same equilibrium position was reached when NADH, rather than NAD^+, was added to the enzyme–substrate solution.

The formation of enzyme-bound NADH was pH dependent (Figure 7B), but not as would be expected if a single group ionizing in the pH range 6–9 controlled K_{int}. A reaction mechanism with two ionizable groups can explain the data (Scheme III). HEAB, EAB, and EAX in Scheme III represent

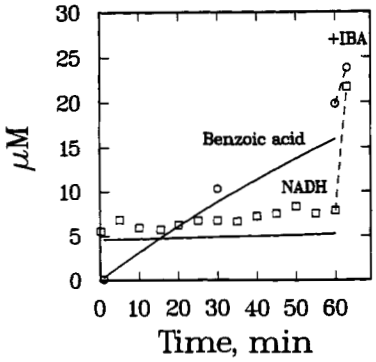

FIGURE 8: Composition of the equilibrium reaction mixture. An equilibrium mixture (see Figure 7) containing 25 μN enzyme, 25 μM NAD^+, 1.0 mM benzyl alcohol, and 0.1 mM benzaldehyde in 46 mM sodium phosphate and 0.25 mM EDTA (pH 7.0, 30 °C) was followed spectrophotometrically at 328 nm at 5-min intervals, and aliquots were removed and quenched at 1, 30, and 60 min of reaction. Isobutyramide (0.1 M) was added after 60 min of reaction time. The aliquots were analyzed by HPLC using the same protocol as for the benzaldehyde oxidation experiments (Figure 6). Parallel blank reactions were made without enzyme and NAD^+ to determine the rate of benzoic acid production due to oxidation in air. A very slow rate of 0.05 μM/min was observed and corrected for. The NADH concentration was calculated from the absorbance at 328 nm. The equilibrium experiment was simulated using the rate constants in Table III, and the lines represent the production of NADH and benzoic acid.

Scheme III

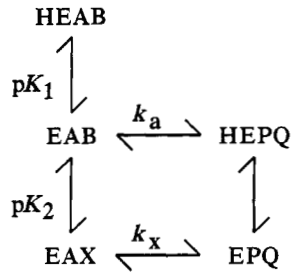

different states of protonation of enzyme complexed with NAD^+ and alcohol, related by the pK values, and k_a and k_x represent microscopic internal equilibrium constants. An equation derived for this mechanism fits the data well (Figure 7B).

Benzoic acid production during the equilibrium experiment was monitored using a protocol similar to that used in studying the dismutation. The results in Figure 8 show that the equilibrium is established very quickly, and the rate of production of the acid is relatively slow. However, as the dismutation removes aldehyde from the reaction, the NADH concentration slowly increases.

The internal equilibrium was also studied by ^{13}C NMR. The signal for [α-^{13}C]benzyl alcohol shifted and broadened upon the addition of NAD^+ to the mixture of enzyme and benzyl alcohol with initial concentrations of 1.4 mN enzyme, 2 mM NAD^+ and 2 mM benzyl alcohol. The ^{13}C signal of benzyl alcohol shifted from 64.81 ppm for the free alcohol to 65.12 ppm in the enzyme–alcohol complex and 65.60 ppm in the ternary complex. No benzaldehyde was detected in the NMR spectrum (196 ppm for free aldehyde). The composition of the reaction mixture after the 12-h NMR experiment was analyzed by UV and HPLC, and the mixture was found to contain 1.1 mM NADH, 1.2 mM benzyl alcohol, and 0.6 mM benzoic acid. No benzaldehyde was detected by HPLC analysis. These results show that the dismutation occurred during the 12-h NMR data acquisition, even at 4 °C, which slows down the dismutation (Anderson & Dahlquist, 1982a).

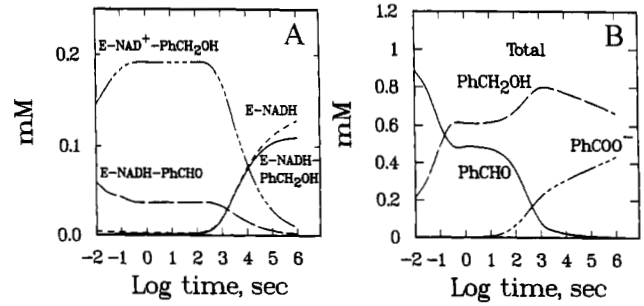

FIGURE 9: Simulations of reactions in crystallization experiments. The crystallizations were simulated using the mechanism in Figure 1 and the kinetic constants given in Table III. The simulation used initial concentrations of 0.25 mN enzyme, 0.65 mM NADH, and 1.1 mM aldehyde. The equilibrium is quickly established between the enzyme–NAD^+–alcohol and enzyme–NADH–aldehyde ternary complexes with the enzyme–NAD^+–alcohol favored about 5 to 1. However, after about 10^3 s, benzaldehyde is substantially oxidized and the concentrations of enzyme–NADH binary and enzyme–NADH–alcohol ternary complexes begin to increase. By 10^6 s, the enzyme is mostly in the enzyme–NADH binary and the enzyme–NADH–alcohol ternary complexes.

Composition of Equilibrium Mixtures Used for X-ray Crystallography. As reported previously (Eklund et al., 1982), reaction mixtures set up to resemble those used for crystallography, with 0.25 mN enzyme, 0.16 mM NADH, 1.1 mM *p*-bromobenzaldehyde, and 5% 2-methyl-2,4-pentanediol, and allowed to incubate at room temperature for 24 days at pH 7, contained about 60% of the coenzyme as NAD^+ (with the rest various degradation products) and 70% of the substrate as benzyl alcohol and 30% as benzoic acid. After incubation for 21 days at pH 7 without enzyme, 85% of the NAD^+ can be recovered, but NADH is mostly converted to NAD^+ and degradation products. These analyses led to the conclusion that the crystals contained predominantly NAD^+ and alcohol. The origin of the acid was not explained, but it could arise from the dismutation.

The concentrations of the various enzyme forms at the pH of the X-ray crystallography studies can now be estimated using the mechanism and the set of rate constants obtained in this study (Figure 9). This is done with the assumptions that *p*-bromobenzyl alcohol has the same reactivity as benzyl alcohol and that the temperature (4 °C) and 2-methyl-2,4-pentanediol used as precipitant (25%) do not affect the relative magnitudes of the rate constants. As determined from the spectrum of the outer dialysate of the reaction mixture (Plapp et al., 1978), the mixture establishes an initial equilibrium position at 0.5 mM NAD^+, 0.5 mM alcohol, 0.37 mM aldehyde, and 0.026 mM NADH. The simulations give comparable concentrations and show that the enzyme would be predominantly complexed with NAD^+ and alcohol during a quasi equilibrium period, as demonstrated by the direct studies of the internal equilibrium (in Figures 7 and 8). Eventually, however, the slow oxidation of aldehyde results in the disappearance of aldehyde and NAD^+ and the formation of alcohol and NADH, so that the abortive complex with NADH and alcohol can form. We also found that reaction of 25 μN enzyme with 21 μM NAD^+ and 1 M methylpentanediol at pH 7 and 25 °C formed 15 μM NADH in 60 min.

DISCUSSION

These studies extend previous knowledge of the reactions catalyzed by liver alcohol dehydrogenase by including pathways with abortive complexes and the dismutation. They also provide an estimate of the internal equilibrium constant and the rate constants for a complete mechanism. The

mechanism is the simplest one that is consistent with the results, but it would be more complicated if kinetically significant intermediates in the interconversion of ternary complexes or isomerizations were included (Sartorius et al., 1987; Sekhar & Plapp, 1990). Nevertheless, the results allow calculation of the concentrations of all known reactants and forms of enzyme at any given set of concentrations, using kinetic simulation.

The common feature of the reactions is the classical ordered bi bi mechanism (steps 1–5 in Figure 1). With low concentrations of benzyl alcohol and benzaldehyde, most of the reaction flux occurs through this pathway. The mechanism with supersaturating concentrations (more than 25 times the K_m value) of benzyl alcohol also includes a pathway involving the abortive enzyme–NADH–benzyl alcohol complex (steps 1–4 and 6–8). For reactions that proceed for more than some minutes, the slow production of benzoic acid occurs through the dismutation pathway (steps 9–11 and 4–2), which irreversibly changes the final reaction composition.

Internal Equilibrium. K_{int} (enzyme–NADH–aldehyde/enzyme–NAD^+–alcohol) estimated from the rate constants in Table III is 0.19. This value agrees closely with the value determined directly by spectrophotometric observations (Figures 7 and 8), which is 0.22–0.25. Because high concentrations of substrates were used in order to drive all enzyme into ternary complexes, about 25% of the absorbance at 328 nm is due to the abortive enzyme–NADH–benzyl alcohol complex, which accounts for the difference in values.

The value for K_{int} is somewhat different than would be calculated simply by comparing the maximal rate constants for the single turnover reactions in the forward and reverse directions: 22/200 = 0.11. These reactions reflect the hydride-transfer steps, as there are significant isotope effects (2–3-fold) with deuterated substrates (McFarland & Bernhard, 1972; Luisi & Bignetti, 1974; Dunn et al., 1979; Sekhar & Plapp, 1990). However, the observed rate constants are transient relaxation constants that are a function of several microscopic rate constants in the mechanism and only approximate the hydride-transfer rates (Pettersson, 1976). If the intrinsic deuterium isotope effect for hydride transfer (step 3) is 6, the isotope effects for the transient reactions are calculated to be about 2.5 for the mechanism in Figure 1. These predictions fit the observed isotope effects and serve to confirm the validity of the simulations.

The UV microspectrophotometry of crystals of binary and ternary complexes of the enzyme suggested that most of the complexes contained 100% of the coenzyme as NADH (Bignetti et al., 1979). The production of NADH in crystals prepared from a solution containing NAD^+ and *p*-bromobenzyl alcohol could be explained by the dismutation (Figure 9), since the crystals had 6 months to react before the microspectrophotometry. On the other hand, crystals prepared with NAD^+ and 2,2,2-trifluoroethanol also contained NADH, and this alcohol is not detectably oxidized by the enzyme. Thus, NADH is forming by another reaction, which is probably due to the oxidation of 2-methyl-2,4-pentanediol, present at 2 M in the crystals. Methylpentanediol is a poor substrate (Plapp et al., 1978) and the equilibrium position favors NADH if the kinetic characteristics of the 2-butanol/2-butanone pair apply (Adolph et al., 1991), but it would not react if the concentrations of competing substrates or inhibitors were sufficiently high. However, before the spectroscopic measurements, the crystals were washed with a buffer containing 30% methylpentanediol and no substrates. Coenzyme does not dissociate from the enzyme under these conditions, but as the concentrations of substrates and inhibitors are decreased, methylpentanediol could react. Thus, NADH can form by various reactions, and further studies are required to determine the composition in the crystals.

Since the dehydrogenase reaction produces a proton and the enzyme–NAD^+–benzyl alcohol complex reacts most rapidly above a pK of 6.4 (Kvassman & Pettersson, 1978), K_{int} could be pH-dependent. The pH dependence (Figure 7B) shows that the reaction is not simply enzyme–NAD^+–alcohol $\rightleftharpoons$ enzyme–NADH–aldehyde + H^+. The data are consistent with the reactions shown in Scheme III, where two ionizable groups control the equilibria. Since the alcohol is ligated to the catalytic zinc and hydrogen-bonded to His-51 through a potential proton relay system, formation of zinc alkoxide or deprotonation of His-51 could influence the internal equilibrium (Eklund et al., 1982). The pK values of 6.5 and 8.1 estimated from the data in Figure 7B describe the system macroscopically, and they are reasonable values for an imidazole and a hydroxyl group bound to zinc. The assignments, however, are not certain, and it has been argued that the pK of 6.5 is controlled by His-51 (Dworschack & Plapp, 1977, Cook & Cleland, 1981) or the alcohol (Kvassman & Pettersson, 1980; Kvassman et al., 1981; Andersson et al., 1984b). The pK of 8.1 has not been observed by other methods, but a pK of 8.6 for dissociation to alkoxide was assumed in order to interpret pH-dependent isotope effects (Cook & Cleland, 1981). The transient reduction of benzaldehyde is independent of pH from 7.9 to 10 (Kvassman & Pettersson, 1978), suggesting that the dissociation of EPQH to EPQ (pK = 7.8, Scheme III) has little effect on hydride transfer. Indeed, the microscopic internal equilibrium constants (k_a and k_x) are not greatly affected by pH, and the pH dependence could arise from indirect effects on enzyme structure.

The K_{int} has also been estimated for the reaction of ethanol and acetaldehyde to be about 1 at pH 7 and 23.5 °C, from very careful spectroscopic measurements and calculations that depended upon knowledge of the dissociation constants of coenzymes (Theorell & Yonetani, 1962). Other work gave an estimate of 0.15 at 25 °C and pH 7.3 (Nambiar et al., 1983). We found a value of about 1 from kinetic simulations of transient reactions with ethanol, 1-propanol, and 1-butanol, and their aldehydes (Sekhar & Plapp, 1990). Dickinson and Dickenson (1978) found a weak pH dependence for yeast alcohol dehydrogenase, with the K_{int} of 0.075 at pH 7.05 rising to 0.15 at pH 8.9.

The estimations of K_{int} for these substrates show that the on-enzyme equilibrium is shifted substantially toward a value of 1. At pH 7, the position is shifted by a factor of 10^3 for benzyl alcohol/benzaldehyde and 10^4 for ethanol/acetaldehyde, as compared to K_{eq}. This shift may arise by quasi boat puckering of the nicotinamide ring (Almarsson et al., 1992), but which interactions between the enzyme and substrates are responsible for this shift are not obvious from inspection of the structures of the enzyme ternary complexes.

Random Pathways. Although the kinetic mechanism of alcohol dehydrogenase is described as compulsory or preferred ordered, it has been suggested that steady-state kinetics is inadequate to establish the extent of reaction by alternative pathways (Andersson et al., 1984a). A random pathway has been proposed for the reaction of NAD^+ with primary and secondary alcohols (Silverstein & Boyer, 1964; Dalziel & Dickinson, 1966a,b; Ainslie & Cleland, 1972). Our stopped-flow results suggest that the enzyme–benzyl alcohol complex does not bind NAD^+ fast enough to contribute significantly to reaction flux. The mechanism derived from these studies

includes an abortive enzyme–NADH–alcohol complex, which can dissociate to enzyme–alcohol, but it does not include a step with binding of NAD^+ to this binary complex. The binding of benzyl alcohol to free enzyme (K_d = 7 mM) is weak relative to binding to the enzyme–NAD^+ complex (26 μM) or the enzyme–NADH complex (0.63 mM). Thus, the binary complex does not affect the slopes of the uncompetitive substrate inhibition pattern (Figure 3). This behavior is in contrast to the results with cyclohexanol, which gave essentially competitive substrate inhibition (Dalziel & Dickinson, 1966b).

The reaction of NADH and benzaldehyde is presented as ordered in Figure 1 since our data can be explained without including an enzyme–aldehyde complex. Such complexes have been demonstrated with 4-(2′-imidazolylazo)benzaldehyde, benzaldehyde, and (dimethylamino)cinnamaldehyde (McFarland et al., 1974; Anderson & Dahlquist, 1980; Andersson et al., 1984a). The azo aldehyde forms a deadend complex that must dissociate before NADH can bind and react, but the enzyme–cinnamaldehyde complex reacts as well as free enzyme does with NADH and produces a random pathway (Andersson et al., 1984a).

Dismutation. The oxidation of aldehydes catalyzed by liver alcohol dehydrogenase has been shown for a number of substrates: formaldehyde, acetaldehyde, butyraldehyde, octanal, heptanal, *p*-(trifluoromethyl)benzaldehyde, and dimethylcinnamaldehyde (Abeles & Lee, 1960; Dalziel & Dickinson, 1965; Henehan & Oppenheimer, 1993; Hinson & Neal, 1975; Battersby et al., 1979; Anderson & Dahlquist, 1982a; Dahl & Dunn, 1984). The kinetic data show that the reaction is catalytically inefficient (V/K) relative to alcohol oxidation. Turnover numbers (V) can be faster than alcohol oxidation due to the coupled, ping-pong mechanism, which bypasses the slow steps of coenzyme dissociation (Figure 1). For instance, V for butyraldehyde oxidation is 14 times faster than for butanol oxidation, but V/K is 100-fold slower (Dalziel & Dickinson, 1965). For benzaldehyde oxidation, V is 2.5-fold and V/K is 4200-fold slower than benzyl alcohol oxidation. The extents of hydration could affect the relative rates. Acetaldehyde is about 50% hydrated, whereas benzaldehyde is about 10% hydrated (Abeles & Lee, 1960; Anderson & Dahlquist, 1982a). Formaldehyde is completely hydrated and is one of the best substrates for the dismutation, and formaldehyde methyl hemiacetal is oxidized to methyl formate (Kendal & Ramanathan, 1952; Abeles & Lee, 1960). Although these dismutation reactions may be relatively slow, their physiological significance cannot be discounted.

Liver alcohol dehydrogenase is a multifunctional enzyme. Simulation of steady-state and transient kinetic data can describe the reactions completely.

ACKNOWLEDGMENT

We thank Dr. James G. Robertson for the KinetAsyst II program used to fit hyperbolic uncompetitive inhibition. The University of Iowa Central Research Facilities provided the SLM 4800C spectrofluorometer, the Bruker WM360 NMR spectrometer, and the Kinetic Instruments stopped-flow apparatus.

REFERENCES

Abeles, R. H., & Lee, H. A., Jr. (1960) *J. Biol. Chem. 235*, 1499–1503.
Adolph, H. W., Maurer, P., Schneider-Bernlöhr, H., Sartorius, C., & Zeppezauer, M. (1991) *Eur. J. Biochem.201*, 615–625.
Ainslie, G. R., Jr., & Cleland, W. W. (1972) *J. Biol. Chem. 247*, 946–951.
Albery, W. J., & Knowles, J. R. (1976) *Biochemistry 15*, 5631–5640.
Almarsson, Ö., Karaman, R., & Bruice, T. C. (1992) *J. Am. Chem. Soc. 114*, 8702-8704.
Anderson, D. C., & Dahlquist, F. W. (1980) *Biochemistry 19*, 5486–5493.
Anderson, D. C., & Dahlquist, F. W. (1982a) *Arch. Biochem. Biophys. 217*, 226-235.
Anderson, D. C., & Dahlquist, F. W. (1982b) *Biochemistry 21*, 3578–3584.
Andersson, P., & Pettersson, G. (1982) *Eur. J. Biochem. 122*, 559–568.
Andersson, P., Kvassman, J., Oldén, B., & Pettersson, G. (1981) *Eur. J. Biochem. 118*, 119–123.
Andersson, P., Kvassman, J., Oldén, B., & Pettersson, G. (1984a) *Eur. J. Biochem. 139*, 519–527.
Andersson, P., Kvassman, J., Oldén, B., & Pettersson, G. (1984b) *Eur. J. Biochem. 144*, 317–324.
Baici, A., & Luisi, P. L. (1977) *J. Mol. Biol. 114*, 267–279.
Barshop, B. A., Wrenn, R. F., & Frieden, C. (1983) *Anal. Biochem. 130*, 134–145.
Battersby, A. R., Buckley, D. G., & Staunton, J. (1979) *J. Chem. Soc., Perkin Trans. 1*, 2559–2562.
Bernhard, S. A., Dunn, M. F., Luisi, P. L., & Schack, P. (1970) *Biochemistry 9*, 185-192.
Bignetti, E., Rossi, G. L., & Zeppezauer, E. (1979) *FEBS Lett. 100*, 17–22.
Brooks, R. L., Shore, J. D., & Gutfreund, H. (1972) *J. Biol. Chem. 247*, 2382–2383.
Burbaum, J. J., & Knowles, J. R. (1989) *Biochemistry 28*, 9306–9317.
Burbaum, J. J., Raines, R. T., Albery, W. J., & Knowles, J. R. (1989) *Biochemistry 28*, 9293–9305.
Cleland, W. W. (1963) *Biochim. Biophys. Acta 67*, 104–137.
Cleland, W. W. (1979) *Methods Enzymol. 63*, 103–138.
Cook, P. F., & Cleland, W. W. (1981) *Biochemistry 20*, 1805–1816.
Dahl, K. H., & Dunn, M. F. (1984) *Biochemistry 23*, 4094–4100.
Dalziel, K. (1963) *J. Biol. Chem. 238*, 2850–2858.
Dalziel, K., & Dickinson, F. M. (1965) *Nature 206*, 255–257.
Dalziel, K., & Dickinson, F. M. (1966a) *Biochem. J. 100*, 34–46.
Dalziel, K., & Dickinson, F. M. (1966b) *Biochem. J. 100*, 491–500.
Dickinson, F. M., & Dickenson, C. J. (1978) *Biochem. J. 171*, 629–637.
Dunn, M. F., Bernhard, S. A., Anderson, D., Copeland, A., Morris, R. G., & Roque, J.-P. (1979) *Biochemistry 18*, 2346–2354.
Dworschack, R. T., & Plapp, B. V. (1977) *Biochemistry 16*, 2716–2725.
Eklund, H., Plapp, B. V., Samama, J.-P., & Brändén, C.-I. (1982) *J. Biol. Chem. 257*, 14349–14358.
Hadorn, M., John, V. A., Meier, F. K., & Dutler, H. (1975) *Eur. J. Biochem. 54*, 65-73.
Henehan, G. T. M., & Oppenheimer, N. J. (1993) *Biochemistry 32*, 735–738.
Hinson, J. A., & Neal, R. A. (1972) *J. Biol. Chem. 247*, 7106–7107.
Hinson, J. A., & Neal, R. A. (1975) *Biochim. Biophys. Acta 384*, 1–11.
Jacobs, J. W., McFarland, J. T., Wainer, I., Jeanmaier, D., Ham, C., Hamm, K., Wnuk, M., & Lam, M. (1974) *Biochemistry 13*, 60–64.
Kamlay, M. T., & Shore, J. D. (1983) *Arch. Biochem. Biophys. 222*, 59–66.
Kendal, L. P., & Ramanathan, A. N. (1952) *Biochem. J. 52*, 430–438.
Klinman, J. P. (1972) *J. Biol. Chem. 247*, 7977–7987.
Kvassman, J., & Pettersson, G. (1976) *Eur. J. Biochem. 69*, 279–287.
Kvassman, J., & Pettersson, G. (1978) *Eur. J. Biochem. 87*, 417–427.

Kvassman, J., & Pettersson, G. (1980) *Eur. J. Biochem. 103*, 565–575.
Kvassman, J., Larsson, A., & Pettersson, G. (1981) *Eur. J. Biochem. 114*, 555–563.
Lee, K. M., Dahlhauser, K. F., & Plapp, B. V. (1988) *Biochemistry 27*, 3528–3532.
Luisi, P. L., & Bignetti, E. (1974) *J. Mol. Biol. 88*, 653–670.
McFarland, J. T., & Bernhard, S. A. (1972) *Biochemistry 11*, 1486–1493.
McFarland, J. T., & Chu, Y.-H. (1975) *Biochemistry 14*, 1140–1146.
McFarland, J. T., Chu, Y. H., & Jacobs, J. W. (1974) *Biochemistry 13*, 65–69.
Nambiar, K. P., Stauffer, D. M., Kolodziej, P. A., & Benner, S. A. (1983) *J. Am. Chem. Soc. 105*, 5886–5890.
Pettersson, G. (1976) *Eur. J. Biochem. 69*, 273–278.
Plapp, B. V. (1970) *J. Biol. Chem. 245*, 1727–1735.
Plapp, B. V., Eklund, H., & Brändén, C.-I. (1978) *J. Mol. Biol. 122*, 23–32.
Plapp, B. V., Green, D. W., Sun, H.-W., Park, D.-H., & Kim, K. (1993) in *Enzymology and Molecular Biology of Carbonyl Metabolism* (Weiner, H., Ed.) Vol. 4, pp 391–400, Plenum Press, New York.
Sartorius, C., Gerber, M., Zeppezauer, M., & Dunn, M. F. (1987) *Biochemistry 26*, 871–882.
Schneider, G., Cedergren-Zeppezauer, E., Knight, S., Eklund, H., & Zeppezauer, M. (1985) *Biochemistry 24*, 7503–7510.
Sekhar, V. C., & Plapp, B. V. (1988) *Biochemistry 27*, 5082–5088.
Sekhar, V. C., & Plapp, B. V. (1990) *Biochemistry 29*, 4289–4295.
Shore, J. D., Gutfreund, H., Brooks, R. L., Santiago, D., & Santiago, P. (1974) *Biochemistry 13*, 4185–4191.
Silverstein, E., & Boyer, P. D. (1964) *J. Biol. Chem. 239*, 3908–3914.
Theorell, H., & Bonnichsen, R. (1951) *Acta Chem. Scand. 5*, 1105–1126
Theorell, H., & Chance, B. (1951) *Acta Chem. Scand. 5*, 1127–1144.
Theorell, H., & McKinley-McKee, J. S. (1961) *Acta Chem. Scand. 15*, 1811–1833.
Theorell, H., & Yonetani, T. (1962) *Arch. Biochem. Biophys. Suppl. 1*, 209–216.
Theorell, H., & Yonetani, T. (1963) *Biochem. Z. 338*, 537–553.
Weidig, C. F., Halvorson, H. R., & Shore, J. D. (1977) *Biochemistry 16*, 2916–2922.
Zimmerle, C. T., & Frieden, C. (1989) *Biochem. J. 258*, 381–387.